

# Kinetics of the reactions of OH(X<sup>2</sup>Π) radicals with 1,3-dioxolane and selected dialkoxy methanes

Carlos M. Freitas Dinis, Harald Geiger and Peter Wiesen\*

Bergische Universität-Gesamthochschule Wuppertal, Physikalische Chemie/FB 9,  
D-42097 Wuppertal, Germany. E-mail: wiesen@physchem.uni-wuppertal.de

Received 3rd January 2001, Accepted 18th May 2001

First published as an Advance Article on the web 12th June 2001

The gas-phase reaction of OH(X<sup>2</sup>Π) radicals with 1,3-dioxolane was investigated in the temperature range 250–550 K. The reactions of OH(X<sup>2</sup>Π) with di-isopropoxy methane (DiPM), di-n-butoxy methane (DnBM) and di-sec-butoxy methane (DsBM) were studied below room temperature down to 250 K. The experiments were carried out in argon, mostly at a total pressure of 400 Torr. A few additional measurements for the reaction OH + 1,3-dioxolane at 50 Torr exhibited that this reaction is independent of total pressure in the range investigated. OH radicals were generated by excimer laser photolysis of H<sub>2</sub>O<sub>2</sub> and were detected by laser-induced fluorescence. For the OH + 1,3-dioxolane reaction, no temperature dependence was observed within the experimental errors. The bimolecular rate coefficient is well described by  $k_{\text{OH}+\text{dioxolane}}(T) = (8.2 \pm 1.3) \times 10^{-12} \text{ cm}^3 \text{ s}^{-1}$ . The rate coefficients measured for the reactions of OH with DiPM, DnBM and DsBM are discussed together with literature data obtained for higher temperatures. The Arrhenius plots for each reaction exhibited concave upward curvatures. From these data, the following Arrhenius expressions were derived (with  $T$  in K and  $E_0$  in kJ mol<sup>-1</sup>):

$$k_{\text{OH}+\text{DiPM}}(T) = (6.2 \pm 8.5) \times 10^{-14} \times (T/298)^{4.3 \pm 1.0} \times \exp[(15.8 \pm 3.2)/RT] \text{ cm}^3 \text{ s}^{-1},$$

$$k_{\text{OH}+\text{DnBM}}(T) = (3.9 \pm 2.8) \times 10^{-13} \times (T/298)^{2.6 \pm 0.5} \times \exp[(13.7 \pm 1.2)/RT] \text{ cm}^3 \text{ s}^{-1},$$

$$k_{\text{OH}+\text{DsBM}}(T) = (1.4 \pm 0.7) \times 10^{-13} \times (T/298)^{3.6 \pm 0.4} \times \exp[(11.5 \pm 0.9)/RT] \text{ cm}^3 \text{ s}^{-1}.$$

The given expressions for the rate coefficients are only valid within the limited temperature range of the present experiments. Since the equations are not theoretically supported, an extrapolation to other temperatures is not allowed.

## 1. Introduction

Ethers are an important class of automotive fuel additives.<sup>1</sup> These compounds enhance the octane level, increase the efficiency of combustion, and reduce the emission of atmospheric pollutants, *e.g.* hydrocarbons, CO and particles.<sup>2–5</sup> The possible industrial application of a large number of new oxygenated compounds such as acetals or esters is currently under discussion;<sup>6</sup> for example, both classes of compound are being considered as alternative solvents.

The compounds under investigation here, 1,3-dioxolane, di-isopropoxy methane (DiPM), di-n-butoxy methane (DnBM) and di-sec-butoxy methane (DsBM), are currently under consideration as potential diesel fuel components to improve the atmospheric properties of the exhaust. It has been shown that the addition of formaldehyde acetals with the general structure R–O–CH<sub>2</sub>–O–R to diesel fuel significantly reduces the emission of particulate matter from diesel engines. However, the widespread use of these organic compounds will result in their release to the atmosphere in significant quantities and thus the potential arises for possible adverse effects on tropospheric chemistry. It is well known, for example, that the reformulation of fuel by several oxygenated VOCs (volatile organic compounds) increases the exhaust concentration of aldehydes<sup>7</sup> and the discovery of methyl *tert*-butyl ether (MTBE) in groundwater and reservoirs used for drinking water<sup>8</sup> has resulted in the prohibition of MTBE as a fuel addi-

tive in California from the beginning of the year 2003.<sup>9</sup> These examples show the necessity to improve the knowledge of the kinetic, mechanistic and environmental behaviour of oxygenated VOCs and their reaction products in the troposphere prior to their widespread application.

In continuation of previous work of our laboratory on the OH radical kinetics of a series of acetals,<sup>10,11</sup> the present study is focused on the reaction of OH radicals with 1,3-dioxolane, which is, in contrast to the usual acetals of the structure R–O–CH<sub>2</sub>–O–R, a cyclic compound. The kinetics of its reaction with OH was studied over a wide temperature range. Furthermore, rate coefficients for the reactions of OH with DiPM, DnBM and DsBM were measured at temperatures below 298 K down to 250 K in order to enhance the temperature range of previous studies, which were carried out in the range 298–700.<sup>10,11</sup>

## 2. Experimental

The excimer laser fluorescence/laser induced fluorescence (ELP/LIF) experimental set-up used in the present work is described in detail elsewhere.<sup>11</sup> Briefly, the focused 248 nm radiation of a Lambda Physik Compex 102 excimer laser with a pulse energy of 20–30 mJ operating at 10 Hz was used to generate OH radicals by photodissociation of H<sub>2</sub>O<sub>2</sub> which was evaporated in argon. Relative OH(X<sup>2</sup>Π) concentrations were monitored by LIF using the Q<sub>1</sub>-branch of the

$A^2\Sigma^+(v'=1) \leftarrow X^2\Pi(v''=0)$  transition at 282 nm and off-resonant detection of the  $A^2\Sigma^+(v'=0) \rightarrow X^2\Pi(v''=0)$  transition at 308 nm. The probe laser was a Lambda Physik system comprising a Scanmate 1 dye laser equipped with an SHG crystal pumped by an LPX 202 excimer laser. For monitoring OH radicals, the frequency-doubled dye laser was operated with Coumarin 153 (Radiant Dyes Chemie) in methanol, yielding typical pulse energies of about 0.5 mJ.

The reaction cell used in the temperature range 250–550 K consisted of a stainless steel cylinder through which the photolysis and the probe laser beams counterpropagated. In the experiments carried out at elevated temperatures, the cell was heated by means of a Ni/Cr (80/20) resistive wire. For studying reactions below room temperature, a coolant fluid was circulated through a jacket surrounding the reaction cell. The temperature in the reaction cell was measured by shielded, calibrated thermocouples and kept constant during the experiments to better than  $\pm 1.5$  K. A detailed description of the reaction cell has been given elsewhere.<sup>12</sup>

The OH fluorescence was observed at right angles to the laser beam through a lens system and an interference filter with a photomultiplier (Thorn EMI 9635QB). The output signal of the photomultiplier was integrated by a boxcar averager (SRS model SR 250), digitised by an AD converter (Rhothron AD 16) and analysed by an ATARI MegaST microcomputer. The time delay between the photolysis laser and the probe dye laser was varied from zero to several ms by means of a digital delay generator (BNC 7010). The time resolution used was 1  $\mu$ s.

All reactions were investigated under pseudo-first order conditions with reactant concentrations at least a hundred times larger than the OH precursor  $H_2O_2$ . All measurements were carried out in slowly flowing gas mixtures with flow rates of  $<0.5$  m s<sup>-1</sup>. The concentrations of the gases were determined from their partial flows measured with calibrated flow meters (Tylan FM 360). In all experiments argon was used as bath gas. The reactants were diluted in argon with ratios of about 1 : 200 for 1,3-dioxolane and about 1 : 600–1 : 6000 for DiPM, DnBM and DsBM and stored in stainless steel cylinders. The exact mixing ratios of the reactant/Ar mixtures were determined by Fourier-transform infrared spectroscopy using calibrated reference spectra.

Argon with a stated purity of 99.998% employed in this work was supplied by Messer Griesheim. DiPM, DnBM and DsBM (Lambiotte & Cie) were distilled twice for purification and carefully degassed before use. 1,3-Dioxolane (Aldrich, >99%) and  $H_2O_2$  (Peroxid-Chemie, 85 wt.%, stabilised) were used without further purification.

### 3. Results and discussion

#### 3.1. Measurements of rate coefficients

From the LIF measurements, relative OH( $X^2\Pi$ ) radical concentrations were measured as a function of the reaction time. As demonstrated in Fig. 1 for the system  $H_2O_2$ /1,3-dioxolane/h $\nu$  as an example, the LIF signal exponentially decayed for all reactant concentrations. In the absence of any reactant, the OH decay was mainly caused by reaction with  $H_2O_2$ , supported by the fact that the measured decay constants were strongly dependent on the  $H_2O_2$  concentration.

The OH decay could be monitored over at least 4 lifetimes. The addition of any reactant caused a more rapid decay of OH radicals. By plotting the natural logarithm of the relative OH concentration as a function of reaction time, pseudo-first order decay constants  $k'$  were calculated from the slope of the individual straight line plots, which were obtained for different reactant concentrations. The  $k'$  values increased proportionally with the concentration of reactant added, as illustrated in Fig. 1.

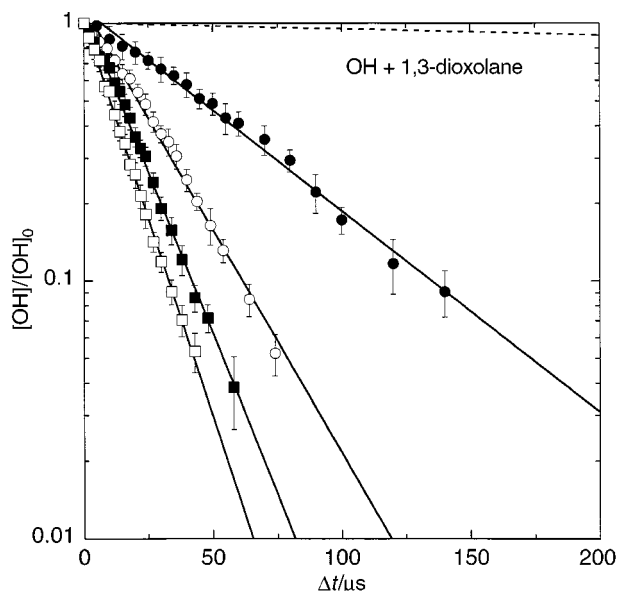


Fig. 1 Semi-logarithmic plot of the OH decay after laser photolysis of  $H_2O_2$  at 400 K in 400 Torr Ar in the presence of different 1,3-dioxolane concentrations ( $10^{15}$  cm<sup>-3</sup>): (●) 2.24; (○) 4.72; (■) 7.03; (□) 9.47. The dashed line represents the OH decay for [reactant] = zero. The error bars reflect  $2\sigma$ .

The bimolecular rate coefficients  $k_{OH+reactant}$  for a given temperature were then obtained by plotting corrected pseudo-first order decay constants  $k'_{corr}$  as a function of the reactant concentration, as shown in Fig. 2 for the reaction OH + 1,3-dioxolane as an example. The  $k'_{corr}$  values were obtained by subtracting the decay constants, which were measured in the absence of reactant, from the corresponding  $k'$  values.

(a) **The reactions of OH radicals with DiPM, DnBM and DsBM.** All experiments with respect to the reactions of OH with DiPM, DnBM and DsBM were carried out at a total pressure of 400 Torr. As reported in earlier publications from our laboratory,<sup>10,11</sup> these reactions were found to be independent of total pressure in the range 50–400 Torr.

In continuation of previous studies on the reactions of OH radicals with DiPM, DnBM and DsBM, which were focused

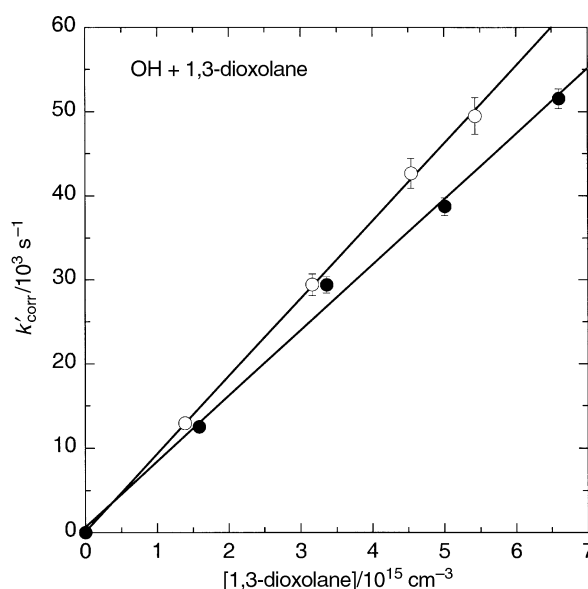


Fig. 2 Plot of pseudo-first-order decay constants  $k'_{corr}$  vs. the concentration of 1,3-dioxolane for 400 K (●) and 550 K (○) at 400 Torr total pressure.

on the temperature range 298–700 K, the rate coefficients for these reactions were measured in the present work for the first time at temperatures below room temperature down to 250 K. Below 250 K, an intensive background radiation at the detection wavelength of 308 nm was observed, which made further signal processing impossible. It is highly certain that below 250 K significant amounts of the reactants, which are all characterised by fairly low vapour pressures, will condense from the gas phase forming aerosols. The background radiation will therefore be due to laser light scattered at the aerosol particles. The data obtained are summarised in Table 1, together with literature values obtained by Thüner *et al.*,<sup>13</sup> who investigated the reactions at room temperature using the relative rate technique. The error limits of the data measured here represent a 90% confidence interval and reflect the statistical precision only. The given rate coefficients are weighted means of at least six  $k$ -values, which were determined in independent experiments using at least 5 different reactant concentrations. For the reaction OH + DnBM, the rate coefficient at 500 K was re-measured. The  $k$ -value of  $(2.58 \pm 0.14) \times 10^{11} \text{ cm}^3 \text{ s}^{-1}$  obtained in the present study is significantly smaller than that of  $(3.85 \pm 0.52) \times 10^{11} \text{ cm}^3 \text{ s}^{-1}$  reported in our previous work.<sup>10</sup> A re-evaluation of the data led to the conclusion that the rate coefficient from the former study was afflicted by a wrong calibration of the DnBM/Ar mixture used, which resulted in a wrong rate coefficient. Accordingly, this value should be deleted from future data evaluations.

**Table 1** Bimolecular rate coefficients for the reactions of OH radicals with DiPM, DnBM, DsBM and 1,3-dioxolane

Reaction	$T$ /K	$k_{\text{exp}}^a$ $/10^{-12} \text{ cm}^3 \text{ s}^{-1}$	Ref. ( $k_{\text{exp}}$ )
OH + 1,3-dioxolane	250 ± 2	7.9 ± 0.4	this work
	270 ± 2	7.9 ± 0.1	this work
	280 ± 2	8.7 ± 0.3	this work
	296 ± 2	7.9 ± 0.4	this work
	296	10.4 ± 1.6	15 <sup>b</sup>
	295	8.8 ± 0.9	15 <sup>c</sup>
	350 ± 2	7.8 ± 0.2	this work
	400 ± 2	7.7 ± 0.3	this work
	498 ± 2	8.7 ± 0.4	this work
	550 ± 2	9.5 ± 0.2	this work
OH + DiPM	250 ± 2	55.2 ± 1.7	this work
	270 ± 2	55.5 ± 2.0	this work
	296 ± 3	34.7 ± 1.8	11
	298	26.3 ± 4.9	13 <sup>b</sup>
	350 ± 4	28.1 ± 1.2	11
	410 ± 2	22.2 ± 1.0	11
	503 ± 2	23.2 ± 2.0	11
	602 ± 7	31.7 ± 3.3	11
OH + DnBM	697 ± 1	34.3 ± 0.8	11
	260 ± 2	49.5 ± 2.7	this work
	270 ± 2	45.6 ± 1.8	this work
	280 ± 2	40.6 ± 3.0	this work
	298 ± 2	33.9 ± 4.6	10
	298	34.7 ± 4.2	13 <sup>b</sup>
	400 ± 2	25.7 ± 3.0	10
	500 ± 2	25.8 ± 1.4	this work
OH + DsBM	600 ± 2	29.4 ± 6.2	10
	710 ± 2	33.1 ± 6.9	10
	261 ± 2	55.0 ± 1.7	this work
	270 ± 2	48.5 ± 1.5	this work
	295 ± 1	42.5 ± 1.3	11
	298	46.8 ± 0.5	13 <sup>b</sup>
	401 ± 1	28.2 ± 2.4	11
	501 ± 5	21.5 ± 3.8	11
	602 ± 4	25.6 ± 2.2	11
	700 ± 5	27.0 ± 4.3	11

<sup>a</sup> Errors in the data from this work reflect a 90% confidence interval.

<sup>b</sup> Relative rate technique. <sup>c</sup> Pulse radiolysis technique.

Fig. 3–5 illustrate the Arrhenius plots for  $k_{\text{OH}+\text{DiPM}}$ ,  $k_{\text{OH}+\text{DnBM}}$  and  $k_{\text{OH}+\text{DsBM}}$ . All data measured in our laboratory using the ELP/LIF technique were plotted. The rate coefficients from the present study measured below room temperature fit well to the previous data, which already exhibited concave upward curvatures of the Arrhenius graphs. For all reactions, the rate coefficients measured below 298 K significantly increased with decreasing temperature. However, the temperature dependencies are not very pronounced. The differences between the highest and the lowest  $k$ -values are not larger than a factor of 2.5 for all reactions. If the three-parameter Arrhenius expression  $k(T) = A \times (T/298)^n \times \exp[E_0/RT]$  is used, the bimolecular rate coefficients of the

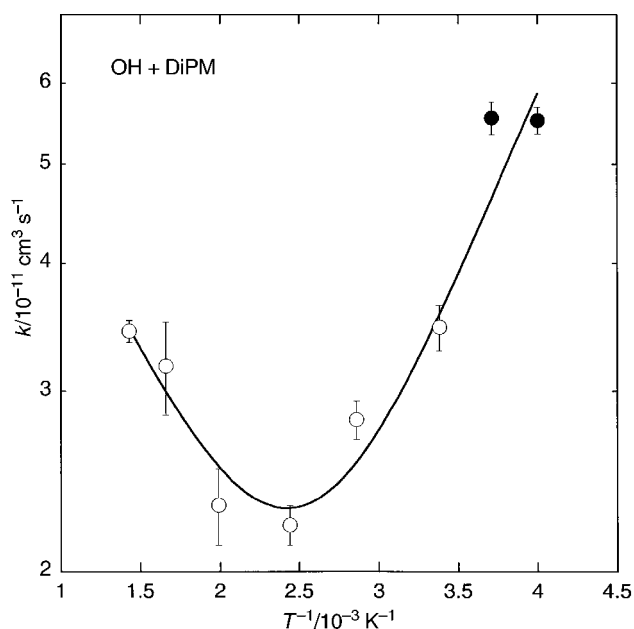


**Fig. 3** Arrhenius plot of the bimolecular rate coefficient  $k_{\text{OH}+\text{DiPM}}$  vs.  $1/T$ . (●) This work; (○) Becker *et al.*<sup>11</sup> (all errors reflect a 90% confidence interval). The solid line corresponds to eqn. (1).

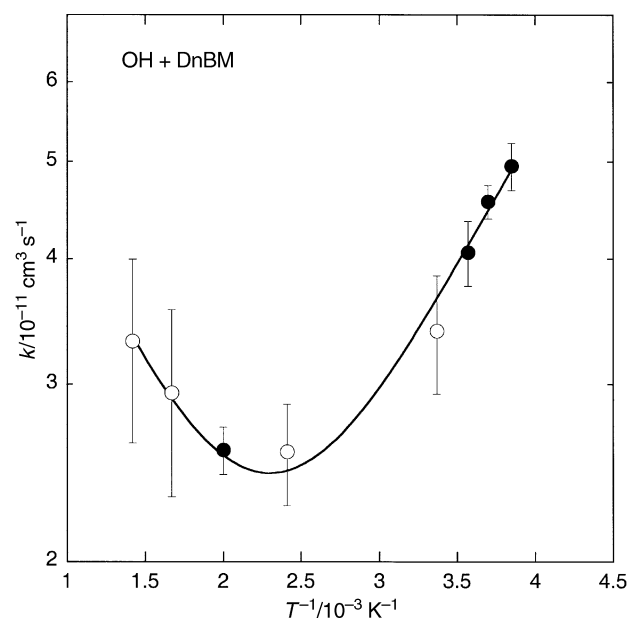


**Fig. 4** Arrhenius plot of the bimolecular rate coefficient  $k_{\text{OH}+\text{DnBM}}$  vs.  $1/T$ . (●) This work; (○) Becker *et al.*<sup>10</sup> (all errors reflect a 90% confidence interval). The solid line corresponds to eqn. (2).

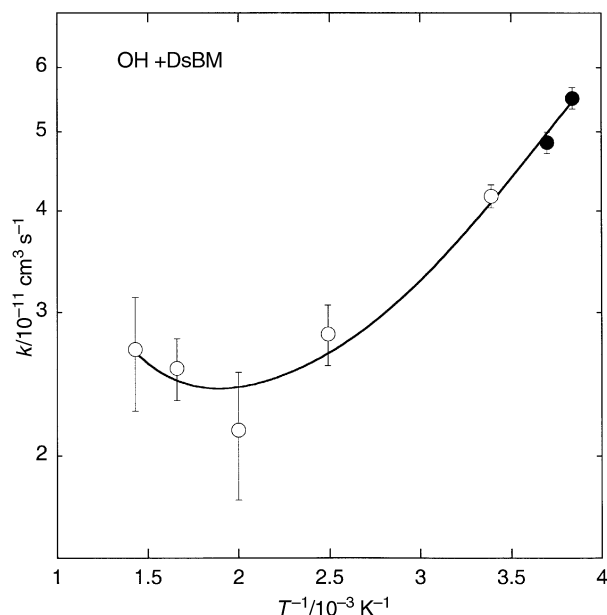


Fig. 5 Arrhenius plot of the bimolecular rate coefficient  $k_{\text{OH}+\text{DsBM}}$  vs.  $1/T$ . (●) This work; (○) Becker *et al.*<sup>11</sup> (all errors reflect a 90% confidence interval). The solid line corresponds to eqn. (3).

reactions of OH radicals with DiPM, DnBM and DsBM, are well described by:

$$k_{\text{OH}+\text{DiPM}}(T) = (6.2 \pm 8.5) \times 10^{-14} \times (T/298)^{4.3 \pm 1.0} \times \exp[(15.8 \pm 3.2)/RT] \text{ cm}^3 \text{ s}^{-1}, \quad (1)$$

$$k_{\text{OH}+\text{DnBM}}(T) = (3.9 \pm 2.8) \times 10^{-13} \times (T/298)^{2.6 \pm 0.5} \times \exp[(13.7 \pm 1.2)/RT] \text{ cm}^3 \text{ s}^{-1}, \quad (2)$$

$$k_{\text{OH}+\text{DsBM}}(T) = (1.4 \pm 0.7) \times 10^{-13} \times (T/298)^{3.6 \pm 0.4} \times \exp[(11.5 \pm 0.9)/RT] \text{ cm}^3 \text{ s}^{-1}. \quad (3)$$

with  $T$  in K and  $E_0$  in  $\text{kJ mol}^{-1}$ . The parameters were obtained by non-linear least-squares fits of the Arrhenius function to the corresponding experimental data. The errors represent  $1\sigma$  and reflect the statistical precision only. In particular the errors for  $A$  appear very high (more than 100% for OH + DiPM), which is due to the scatter of the experimental data, obviously caused by the fairly weak temperature dependences of the reactions. The given expressions for the rate coefficients are only valid within the limited temperature range of the present experiments. Since the equations are not theoretically supported, an extrapolation to other temperatures is not allowed.

Possible reasons for the concave upward curvatures of the Arrhenius plots for all 3 reactions investigated have already been discussed in the literature.<sup>11,14</sup> Porter *et al.*<sup>14</sup> proposed a transition state including a five-membered ring for the OH attack. The stability of such a structure will increase with decreasing temperature, which could explain the decrease of the rate coefficient with increasing temperature. Above a given temperature, the reaction will proceed as a typical abstraction reaction and the Arrhenius plot will exhibit a positive temperature dependence. However, a temperature dependence such as observed for the acetals investigated here is normally found for multi-channel reactions. In contrast, it is highly certain that the OH reactions with acetals of the type  $\text{R}-\text{O}-\text{CH}_2-\text{O}-\text{R}$  will proceed as pure abstraction reactions, similar to alkanes, which has been confirmed by several product studies.<sup>15–18</sup> Regarding the present work, it must be stated that the temperature dependences observed are weak, with variation of the highest and lowest rate coefficients for each reaction of a factor of about 2. In conclusion, the reasons

for the Arrhenius plots observed for the reactions of OH with DiPM, DnBM and DsBM remain unclear. It has to be admitted that for a quantitative interpretation of the data the temperature range in the present investigations might be too narrow. In future experiments, the extension of the temperature to higher and lower  $T$ -values would offer a much better database.

**(b) The reaction of OH radicals with 1,3-dioxolane.** For the reaction of OH radicals with 1,3-dioxolane, almost all experiments were carried out at a total pressure of 400 Torr. A few additional studies of the system  $\text{H}_2\text{O}_2/1,3\text{-dioxolane}/h\nu$  performed at 50 Torr and 298 K yielded similar results to those obtained at 400 Torr, indicating that the reaction of OH radicals with 1,3-dioxolane is independent of pressure within this range.

The bimolecular rate coefficient for the reaction of OH radicals with 1,3-dioxolane was measured for the first time as a function of temperature in the range 250–550 K. The rate coefficients obtained are summarised in Table 1. This table also includes data measured by Sauer *et al.*<sup>15</sup> using different experimental techniques at room temperature. The error limits of the rate coefficients measured in the present work represent a 90% confidence interval and reflect the statistical precision only. The given rate coefficients are weighted means of at least five  $k$ -values which were determined in independent measurements using at least 5 different concentrations of 1,3-dioxolane. As discussed above for the other reactants investigated, also during the measurements in the system  $\text{H}_2\text{O}_2/1,3\text{-dioxolane}/h\nu$  an intensive background radiation at the probe laser wavelength appeared for temperatures below 250 K. Therefore, it was not possible to expand the temperature range to lower values. Above 550 K, the shapes of the OH decay curves were found to be non-exponential. It can be expected that pyrolysis of 1,3-dioxolane will appear at higher temperatures. The pyrolysis fragments formed will then become a significant sink for OH radicals, which will influence the pseudo-first order conditions assumed for the reaction system. In addition, emissions in the range of the OH detection wavelength of 308 nm possibly caused by excited pyrolysis products might interfere with the OH LIF signal. Accordingly, rate coefficients for the reaction of OH + 1,3-dioxolane were not determined for temperatures  $> 550$  K.

Within the experimental errors, the reaction was found to be independent of temperature. From the rate coefficients determined in the present work (see Table 1), a mean value of  $k_{\text{OH}+\text{dioxolane}} = (8.2 \pm 1.3) \times 10^{-12} \text{ cm}^3 \text{ s}^{-1}$  was calculated (error =  $2\sigma$ ), which is, within the errors, in good agreement with the  $k$ -values of  $(10.4 \pm 1.6) \times 10^{-12} \text{ cm}^3 \text{ s}^{-1}$  and  $(8.8 \pm 0.9) \times 10^{-12} \text{ cm}^3 \text{ s}^{-1}$ , obtained by Sauer *et al.*<sup>15</sup> from relative rate and pulse radiolysis studies, respectively.

## Summary

The reactions of  $\text{OH}(\text{X}^2\text{II})$  with DiPM, DnBM and DsBM were studied at temperatures below 298 K down to 250 K by excimer laser photolysis/laser-induced fluorescence. Within the investigated range, only weak temperature dependences of the bimolecular rate coefficients were observed. For all reactions, the rate coefficient increased with decreasing temperature. The data obtained here were analysed and discussed together with  $k$ -values previously published. For all compounds investigated, the Arrhenius plots exhibit concave upward curvatures with minima at about 500 K. The reasons for this temperature behaviour of the reactions investigated remain unclear, since the Arrhenius plots obtained are more typical of multi-channel reactions. However, for the reactions of OH with acetals of the type  $\text{R}-\text{O}-\text{CH}_2-\text{O}-\text{R}$ , a simple abstraction mechanism, in analogy to alkane reactions, is

highly certain. Since the temperature range covered in the present study is fairly small with respect to the weak Arrhenius behaviour observed, the extension of the temperature range in future investigations might yield data, which allow a more quantitative interpretation of the reactions.

The reaction rate coefficient for  $\text{OH}(\text{X}^2\Pi) + 1,3\text{-dioxolane}$  was studied for the first time as a function of temperature in the range 250–550 K. The reaction was found to be independent of total pressure in the range 50–400 Torr and also showed no temperature dependence within the range investigated. The averaged rate coefficient determined in the present work is in good agreement with literature data obtained at room temperature.

## Acknowledgements

The financial support for this work by the German “Bundesministerium für Bildung und Forschung (BMBF)”, project “Förderschwerpunkt Troposphärenforschung (TFS)”, contract no. 07TFS30 and the “Ministerium für Schule, Wissenschaft und Forschung des Landes Nordrhein-Westfalen” (MSWWF) is gratefully acknowledged. The authors would like to thank Lambiotte & Cie for the supply of DiPM, DnBM and DsBM.

## References

- 1 C. P. Hälsig, R. Gregory and T. Peacock, *Spec. Publ.-R. Soc. Chem.*, 1991, **97**, 311.
- 2 L. J. Dolislager, *J. Air. Waste Manage. Assoc.*, 1997, **47**, 775.
- 3 H. Guttman and K. P. Schug, *SAE Technical Paper Series*, No. 900274, Society of Automotive Engineers, Warrendale, PA, USA, 1990.
- 4 CONCAWE Automotive Emissions Management Group, *Report No. 2/95*, Brussels, Belgium, 1995.
- 5 L. Dodge and D. W. Naegeli, *Final Report No. NREL/-TP-425-6345*, National Renewable Energy Laboratory, Golden, CO, USA, 1994.
- 6 T. J. Wallington, M. D. Hurley, J. C. Ball, A. M. Straccia, J. Platz, L. K. Christensen, J. Sehested and O. J. Nielsen, *J. Phys. Chem. A*, 1997, **101**, 5302.
- 7 R. M. Reuter, J. D. Benson, V. R. Burnes, R. A. Gorse, A. M. Hochhauser, W. J. Koehl, L. J. Painter, B. H. Rippon and J. A. Rutherford, *SAE Technical Paper Series*, No. 920326, Society of Automotive Engineers, Warrendale, PA, USA, 1992.
- 8 P. J. Squillace, J. S. Zogorski, W. G. Wilber and C. V. Price, *Environ. Sci. Technol.*, 1996, **30**, 1721.
- 9 P. M. Morse, *Chem. Eng. News*, 1999, **77**, 26.
- 10 K. H. Becker, C. Dinis, H. Geiger and P. Wiesen, *Chem. Phys. Lett.*, 1999, **300**, 460.
- 11 K. H. Becker, C. M. Freitas Dinis, H. Geiger and P. Wiesen, *Phys. Chem. Chem. Phys.*, 1999, **1**, 4721.
- 12 K. H. Becker, B. Engelhardt, H. Geiger, R. Kurtenbach and P. Wiesen, *Chem. Phys. Lett.*, 1993, **210**, 135.
- 13 L. P. Thüner, I. Barnes, T. Maurer, C. G. Sauer and K. H. Becker, *Int. J. Chem. Kinet.*, 1999, **31**, 797.
- 14 E. Porter, J. Wenger, J. Treacy, H. Sidebottom, A. Mellouki, S. Téton and G. Le Bras, *J. Phys. Chem. A*, 1997, **101**, 5570.
- 15 C. Sauer, I. Barnes, K. H. Becker, H. Geiger, T. J. Wallington, L. K. Christensen, J. Platz and O. J. Nielsen, *J. Phys. Chem. A*, 1999, **103**, 5959.
- 16 T. Maurer, H. Hass, I. Barnes and K. H. Becker, *J. Phys. Chem. A*, 1999, **103**, 5032.
- 17 J. Platz, L. K. Christensen, J. Sehested, O. J. Nielsen, T. J. Wallington, C. Sauer, I. Barnes, K. H. Becker and R. Vogt, *J. Phys. Chem. A*, 1998, **102**, 4829.
- 18 H. Geiger, I. Barnes, K. H. Becker, B. Bohn, T. Brauers, B. Donner, H.-P. Dorn, M. Elend, C. M. Freitas Dinis, D. Grossmann, H. Hass, H. Hein, A. Hoffmann, L. Hoppe, F. Hülsemann, D. Kley, B. Klotz, H. G. Libuda, T. Maurer, D. Mihelcic, G. K. Moortgat, R. Olariu, P. Neeb, D. Poppe, L. Ruppert, C. G. Sauer, O. Shestakov, H. Somnitz, W. R. Stockwell, L. P. Thüner, A. Wahner, P. Wiesen, F. Zabel, R. Zellner and C. Zetzsch, *J. Atmos. Chem.*, 2001, in press.